



Breaking the Theoretical Scaling Limit for Predicting Quasiparticle Energies: The Stochastic GW Approach

Daniel Neuhauser,¹ Yi Gao,¹ Christopher Arntsen,¹ Cyrus Karshenas,¹ Eran Rabani,² and Roi Baer³

¹Department of Chemistry, University of California at Los Angeles, California 90095, USA

²School of Chemistry, The Sackler Faculty of Exact Sciences, Tel Aviv University, Tel Aviv 69978, Israel

³Fritz Haber Center for Molecular Dynamics, Institute of Chemistry, The Hebrew University of Jerusalem, Jerusalem 91904, Israel

(Received 19 February 2014; published 11 August 2014)

We develop a formalism to calculate the quasiparticle energy within the *GW* many-body perturbation correction to the density functional theory. The occupied and virtual orbitals of the Kohn-Sham Hamiltonian are replaced by stochastic orbitals used to evaluate the Green function G , the polarization potential W , and, thereby, the *GW* self-energy. The stochastic *GW* (s*GW*) formalism relies on novel theoretical concepts such as stochastic time-dependent Hartree propagation, stochastic matrix compression, and spatial or temporal stochastic decoupling techniques. Beyond the theoretical interest, the formalism enables *linear scaling GW* calculations breaking the theoretical scaling limit for *GW* as well as circumventing the need for energy cutoff approximations. We illustrate the method for silicon nanocrystals of varying sizes with $N_e > 3000$ electrons.

DOI: 10.1103/PhysRevLett.113.076402

PACS numbers: 71.10.-w, 71.15.Qe, 74.25.Jb

The *GW* approximation [1,2] to many-body perturbation theory (MBPT) [3] offers a reliable and accessible theory for quasiparticles (QPs) and their energies [2,4–18], enabling estimation of electronic excitations [19–25], quantum conductance [26–30], and level alignment in hybrid systems [31,32]. Practical use of the *GW* approximation for large systems is severely limited because of the steep CPU and memory requirements as system size increases. The most computationally intensive element in the *GW* method, the calculation of the polarization potential (the screened Coulomb interaction), involves an algorithmic complexity that scales as the fourth power of the system size [33,34]. Various approaches have been developed to reduce the computational bottlenecks of the *GW* approach [8,18,23,33–37]. Despite these advances, *GW* calculations are still quite expensive for many of the intended applications in the fields of materials science, surface science, and nanoscience.

In this Letter we develop a stochastic, orbital-less, formalism for the *GW* theory, unique in that it does not reference occupied or virtual orbitals and orbital energies of the Kohn-Sham (KS) Hamiltonian. While the approach is inspired by recent developments in electronic structure theory using stochastic orbitals [38–42], it introduces three powerful and basic notions: Stochastic decoupling, stochastic matrix compression, and stochastic time-dependent Hartree (sTDH) propagation. The result is a stochastic formulation of the *GW* approximation, where the QP energies become random variables sampled from a distribution with a mean equal to the exact *GW* energies and a statistical error proportional to the inverse square root of the number of stochastic orbitals (iterations, I_{sGW}).

We illustrate the s*GW* formalism for silicon nanocrystals (NCs) with varying sizes and band gaps [43,44] and

demonstrate that the CPU time and memory required by s*GW* scales nearly linearly with system size, thereby providing the means to study QPs excitations in large systems of experimental and technological interest.

In the reformulation of the *GW* approach, we treat the QP energy ($\epsilon_{QP} = \hbar\omega_{QP}$) as a perturbative correction to the KS energy [2,5]:

$$\epsilon_{QP}(\epsilon) = \epsilon + \tilde{\Sigma}^P(\omega_{QP}; \epsilon) + \Sigma^X(\epsilon) - \Sigma^{XC}(\epsilon). \quad (1)$$

We view the KS energy ϵ as a variable (rather than an eigenvalue) and the actual value we use is determined from the density of states of the KS Hamiltonian available from the stochastic density functional theory (sDFT) calculation [41]. For each value of ϵ one needs to evaluate the self-energy in Eq. (1) given by the sum of the self-energy terms

$$\begin{aligned} \Sigma^P(t; \epsilon) &= \frac{1}{Q(\epsilon)} \text{tr}[f_\sigma(\hat{h}_{KS} - \epsilon)^2 \hat{\Sigma}^P(t; \epsilon)], \\ \Sigma^X(\epsilon) &= \frac{1}{Q(\epsilon)} \text{tr}[f_\sigma(\hat{h}_{KS} - \epsilon)^2 \hat{\Sigma}^X], \\ \Sigma^{XC}(\epsilon) &= \frac{1}{Q(\epsilon)} \text{tr}[f_\sigma(\hat{h}_{KS} - \epsilon)^2 v_{XC}]. \end{aligned} \quad (2)$$

The frequency domain polarization self-energy $\tilde{\Sigma}^P(\omega, \epsilon)$ is given in terms of the Fourier transform of the time domain counterpart $\Sigma^P(t, \epsilon)$. $\Sigma^X(\epsilon)$ and $\Sigma^{XC}(\epsilon)$ are the exchange and exchange-correlation self-energies, respectively, and $Q(\epsilon) = \text{tr}[f_\sigma(\hat{h}_{KS} - \epsilon)^2]$ is a normalization factor. In the above, $v_{XC}(\mathbf{r})$ is the exchange-correlation potential of the KS DFT Hamiltonian \hat{h}_{KS} and $f_\sigma(\epsilon) = e^{-\epsilon^2/2\sigma^2}$ is an energy filter function of width σ [45]. $\Sigma^X(\epsilon)$, $\Sigma^{XC}(\epsilon)$,

and $Q(\varepsilon)$ can be calculated using a linear-scaling stochastic approach [46].

In the GW approximation, the most demanding calculation involves the polarization self-energy, formally given by [2]:

$$\begin{aligned}\Sigma^P(\mathbf{r}_1, \mathbf{r}_2, t; \varepsilon) &= \langle \mathbf{r}_1 | \hat{\Sigma}^P(t; \varepsilon) | \mathbf{r}_2 \rangle \\ &= i\hbar G_0(\mathbf{r}_1, \mathbf{r}_2, t) W^P(\mathbf{r}_1, \mathbf{r}_2, t; \varepsilon),\end{aligned}\quad (3)$$

where

$$i\hbar G_0(\mathbf{r}_1, \mathbf{r}_2, t) \equiv \langle \mathbf{r}_1 | e^{-i\hat{h}_{\text{KS}}t/\hbar} \hat{P}_\mu(t) | \mathbf{r}_2 \rangle \quad (4)$$

is the Green function and

$$W^P(\mathbf{r}_1, \mathbf{r}_2, t; \varepsilon) \equiv \langle \mathbf{r}_1 | u_C \otimes \chi(t; \varepsilon) \otimes u_C | \mathbf{r}_2 \rangle \quad (5)$$

is the polarization potential. In the above equations, $\hat{P}_\mu(t) \equiv [\theta(t) - \theta_\beta(\mu - \hat{h}_{\text{KS}})]$, $\theta(t)$ and $\theta_\beta(E) = \frac{1}{2}[1 + \text{erf}(\beta E)]$ are the Heaviside and smoothed-Heaviside functions, respectively, μ is the chemical potential, $u_C(|\mathbf{r}_1 - \mathbf{r}_2|) = (e^2/4\pi)\epsilon_0/|\mathbf{r}_1 - \mathbf{r}_2|$ is the bare Coulomb potential, and $\chi(\mathbf{r}_1, \mathbf{r}_2, t; \varepsilon)$ is the time-ordered density-density correlation function [3]. The symbol \otimes represents a space convolution.

Instead of performing the trace operations in Eqs. (2)–(5) using a full basis, which for a large system is prohibitive, we use real stochastic orbitals $\phi(\mathbf{r})$ [47–50] for which formally $\mathbf{1} = \langle |\phi\rangle\langle\phi| \rangle_\phi$, where $\langle \dots \rangle_\phi$ denotes a statistical average over ϕ . The choice of $\phi(\mathbf{r})$ satisfying these requirements is not unique. The form used here assigns a value of $\pm h^{-3/2}$ at each grid point with equal probability, where h is the grid spacing. This allows us to rewrite the self-energy in Eq. (2) as

$$\Sigma^P(t; \varepsilon) = \left\langle \iint \phi_\varepsilon(\mathbf{r}_1) \Sigma^P(\mathbf{r}_1, \mathbf{r}_2, t; \varepsilon) \phi(\mathbf{r}_2) d^3r_1 d^3r_2 \right\rangle_\phi, \quad (6)$$

where $|\phi_\varepsilon\rangle = f_\sigma(\hat{h}_{\text{KS}} - \varepsilon)|\phi\rangle$ is the corresponding filtered state at energy ε , which can be obtained by a Chebyshev expansion of the Gaussian function with σ chosen as a small parameter [51,52]. We note in passing that the Chebyshev method enables to simultaneously obtain $\Sigma^P(t; \varepsilon)$ for several values of ε [53].

To obtain $\Sigma^P(\mathbf{r}_1, \mathbf{r}_2, t; \varepsilon)$ in Eq. (6) we need to calculate the noninteracting Green function $i\hbar G_0(\mathbf{r}_1, \mathbf{r}_2, t)$ in Eq. (4) and the polarization potential $W^P(\mathbf{r}_1, \mathbf{r}_2, t; \varepsilon)$ in Eq. (5). For the former, we introduce an additional set of real stochastic orbitals, $\zeta(\mathbf{r})$, and describe it as a stochastic average

$$i\hbar G_0(\mathbf{r}_1, \mathbf{r}_2, t) = \langle \zeta_\mu(\mathbf{r}_1, t) \zeta(\mathbf{r}_2) \rangle_\zeta, \quad (7)$$

where $\zeta_\mu(\mathbf{r}, t) = \langle \mathbf{r} | e^{-i\hat{h}_{\text{KS}}t/\hbar} \hat{P}_\mu(t) | \zeta \rangle$ is a “propagated-projected” stochastic orbital which can be obtained by a Chebyshev expansion of the function $e^{-i\epsilon t/\hbar}[\theta(t) - \theta_\beta(\varepsilon - \mu)]$ [51,52]. One appealing advantage of the stochastic form of Eq. (7) is that it provides a compact representation for $G_0(\mathbf{r}_1, \mathbf{r}_2, t)$, equivalent to matrix

compression, where \mathbf{r}_1 and \mathbf{r}_2 are decoupled. This allows a drastic simplification of the representation of the polarization self-energy obtained by combining Eqs. (6) and (7):

$$\Sigma^P(t; \varepsilon) = \langle \langle \phi_\varepsilon \zeta_\mu(t)^* | u_C \otimes \chi(t) \otimes u_C | \zeta \phi \rangle \rangle_{\phi\zeta}. \quad (8)$$

Next, we employ a temporal decoupling scheme by introducing an additional set of real stochastic orbitals $\psi(\mathbf{r})$:

$$\Sigma^P(t; \varepsilon) = \langle \langle \phi_\varepsilon \zeta_\mu(t)^* | \psi \rangle \langle \psi | u_C \otimes \chi(t) \otimes u_C | \zeta \phi \rangle \rangle_{\phi\zeta\psi}, \quad (9)$$

which allows us to disassociate the two temporal terms $\langle \phi_\varepsilon \zeta_\mu(t)^* | \psi \rangle$ and $\langle \psi | u_C \otimes \chi(t) \otimes u_C | \zeta \phi \rangle$. Note that the average $\langle \dots \rangle_{\phi\zeta\psi}$ in Eq. (9) is performed over I_{sGW} pairs of ϕ and ζ stochastic orbitals, and for each such pair we use a different set of N_ψ stochastic ψ 's. The term $\langle \phi_\varepsilon \zeta_\mu(t)^* | \psi \rangle$ is straightforward to obtain while $\langle \psi | u_C \otimes \chi(t) \otimes u_C | \zeta \phi \rangle$ is determined from the time-retarded polarization potential, $\langle \psi | u_C \otimes \chi^r(t) \otimes u_C | \zeta \phi \rangle$, calculated from the linear response relation:

$$\langle \psi | u_C \otimes \chi^r(t) \otimes u_C | \zeta \phi \rangle = \langle \psi | u_C | \delta n(t) \rangle, \quad (10)$$

where $\delta n(\mathbf{r}, t)$ is the causal density response to the impulsive perturbation $\delta v(\mathbf{r}, t) = \langle \mathbf{r} | u_C | \zeta \phi \rangle \delta(t)$ calculated by the time-dependent Hartree (TDH) approach [54–56]. Alternatively, a full time-dependent (TD) density functional theory (DFT) [57] is often found to yield better QP energies than the TDH propagation [21]. Once the retarded response $\langle \psi | u_C | \delta n(t) \rangle$ is calculated and stored for each time t , the corresponding time-ordered response $\langle \psi | u_C \otimes \chi(t) \otimes u_C | \zeta \phi \rangle$ is obtained by a standard transformation [58].

The TDH (or TD DFT) propagation is usually performed using the full set of occupied KS eigenfunctions, but we deliberately avoid these in our formulation. Instead, we introduce, once again, a stochastic way to perform the TDH or TD DFT propagation, where a new set of N_ϕ occupied projected stochastic orbitals $\varphi_\mu(\mathbf{r}, 0) = \langle \mathbf{r} | \theta(\mu - \hat{h}_{\text{KS}}) | \varphi \rangle$ are used [as before, $\varphi(\mathbf{r})$ are real random orbitals for which $\mathbf{1} = \langle |\varphi\rangle\langle\varphi| \rangle_\varphi$]. The so-called sTDH (or sTD DFT) propagation is carried out identically to a TDH propagation, except that one propagates only the N_ϕ stochastic orbitals at each time step (rather than all occupied orbitals), and the density is calculated as $n(\mathbf{r}, t) = \langle |\varphi(\mathbf{r}, t)|^2 \rangle_\varphi$ from which the Hartree potential is updated in the usual way [59]. We verified that for a given accuracy the number of propagated orbitals N_ϕ does not increase (and actually somewhat decreases) with system size [60]. This suggests that the computational complexity (storage and computational time) of the sTDH (or sTD DFT) step scales linearly with system size.

We validate our formalism by first applying it to a small model system where a deterministic GW calculation is available as a benchmark [61]. In Fig. 1 we show the estimates for the real part of the polarization self-energy, obtained by both the deterministic and the stochastic

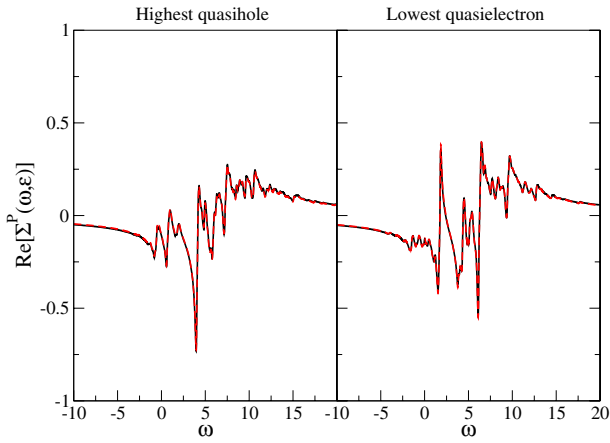


FIG. 1 (color online). Comparison of the stochastic (dashed red) and deterministic (black) estimates of the real part of the polarization self-energy $\tilde{\Sigma}^P(\omega, \epsilon)$ for the 14 electron benchmark model corresponding to the highest quasihole and lowest quasidelectron levels. Frequency scale in atomic units.

methods. The stochastic calculation employed a large number of iterations ($I_{sGW} = 10000$), to achieve small statistical errors. The agreement between the results of the two calculations for all relevant frequencies as seen in Fig. 1 is impressive for both the highest quasihole and lowest quasidelectron levels, validating the stochastic formulation.

Next, we performed a set of *sGW* calculations for a series of hydrogen passivated silicon NCs as detailed in Table I. The *sDFT* method [41] was used to generate the Kohn-Sham Hamiltonian within the local density approximation (LDA). The calculations employed a real-space grid of spacing $h = 0.6a_0$, the Troullier-Martins norm-conserving pseudopotentials [62], and fast Fourier transforms for implementing the kinetic and Hartree energies. The CPU time needed to converge the *sDFT* to a statistical error in the total energy per electron of about 10 meV was ≈ 5000 h for the entire range of systems studied.

In the lower panel of Fig. 2 we plot the QP energies of the highest quasihole and lowest quasidelectron levels for the silicon NCs. We have used $I_{sGW} = 1000$ stochastic iterations, each one involving one pair of random ϕ and ζ orbitals, and a set of $N_\psi = 100$ random ψ orbitals. As can

be seen, the statistical error in the values of the QP energies is very small (< 0.1 eV) and can be reduced by increasing I_{sGW} . The quasihole (quasidelectron) energy increases (decreases) with system size due to the quantum confinement effect. The quasiparticle energies tend to plateau and approach the bulk value as the size of the NC increases. The onset of the plateau for the quasidelectron seems to exceed the size of the systems studied. This is consistent with the fact that the effective mass of the electron is smaller than that of the hole. The middle panel of Fig. 2 shows the QP energy difference from the KS values for the holes and electrons. Larger deviations are observed for small NCs in the strong confinement regime. The corrections for the holes are larger than that for the electrons. This is rather surprising, given that for small systems, the error in the frontier orbital energies in KS DFT within LDA should be divided equally between the electron and the hole [63,64].

The upper panel of Fig. 2 shows the CPU time scaling of the entire *sGW* approach for the combined calculation of $\Sigma^X(\epsilon)$, $\Sigma^{XC}(\epsilon)$, and $\Sigma^P(t; \epsilon)$. The scaling is nearly linear with the number of electrons breaking the quadratic theoretical limit. This near-linear scaling behavior kicks in already for the smallest system studied and, therefore, the stochastic method outperforms the ordinary $O(N^4)$ *GW* approach for all systems studied beyond SiH_4 . It is important to note that for almost the entire range of NC sizes the *sGW* calculations were cheaper than the *sDFT*.

We have also tested the *sGW* performance on phenyl-C61-butyric acid methyl ester (PCBM), a large nonsymmetric system. We obtained $\epsilon_{QP} = 7.1 \pm 0.1$ eV for the hole and $\epsilon_{QP} = 3.4 \pm 0.1$ eV for the electron using $I = 600$ iterations. These results can be compared to the experimental results for the ionization potential $E_{IP} = 7.17$ eV and electron affinity $E_{EA} = 2.63$ eV [65,66]. The agreement for the electron affinity can be improved by replacing the RPA screening with TD DFT screening [67], which gives $\epsilon_{QP} = 2.5 \pm 0.1$ eV for the electron. The error per iteration is thus similar to that of the symmetric silicon nanocrystalline systems.

In conclusion, we have reformulated the *GW* approximation to MBPT for QP energies as a stochastic process without directly referring to KS eigenstates (or,

TABLE I. The number of electrons (N_e), size of grid (N_g), number of *sDFT* iterations (I_{sDFT}), number of stochastic orbitals in *sTD DFT* (N_ϕ), the value of $\beta_{GW}^{-1}(E_h)$ in the *sGW* calculation, and the resulting QP energy gap (E_{gap}^{QP}) compared to GW_f and self-consistent-field energy differences (ΔSCF) calculations.

System	N_e	N_g	I_{sDFT}	N_ϕ	β_{GW}^{-1}	E_{gap}^{QP} (eV)		
						<i>sGW</i>	GW_f	ΔSCF
$\text{Si}_{35}\text{H}_{36}$	176	60^3	3000	16	0.020	6.2	7.0 ^a	6.2 ^a
$\text{Si}_{87}\text{H}_{76}$	424	64^3	1600	16	0.012	4.8		
$\text{Si}_{147}\text{H}_{100}$	688	70^3	800	16	0.010	4.1	5.0 ^a	4.1 ^a
$\text{Si}_{353}\text{H}_{196}$	1608	90^3	400	16	0.008	3.0		2.9 ^b
$\text{Si}_{705}\text{H}_{300}$	3120	108^3	200	16	0.007	2.2		2.4 ^b

^aFrom Ref. [21].

^bFrom Ref. [44].

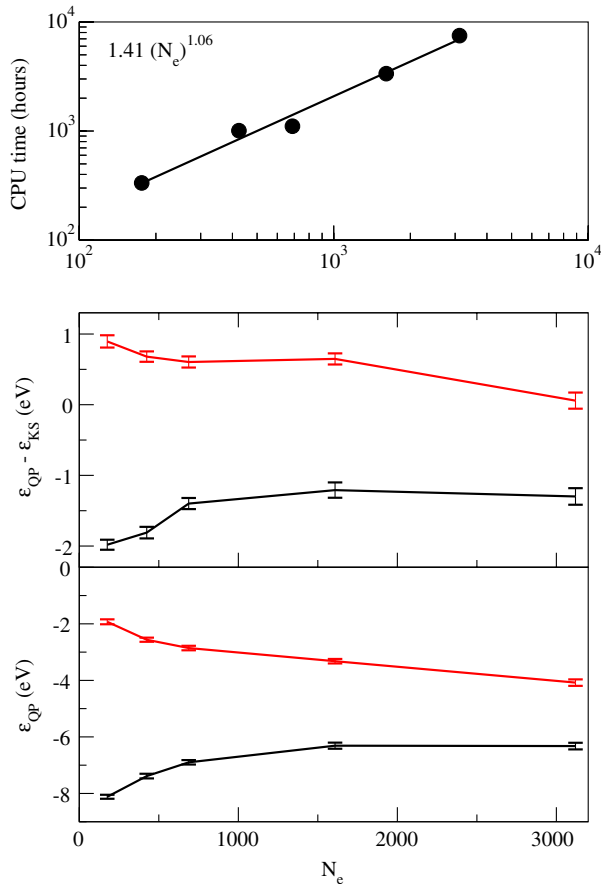


FIG. 2 (color online). Lower panel: QP energies for the highest quasihole (black) and lowest quasihole (red) levels. Middle panel: QP energy difference from the KS energy for the highest quasihole (black) and lowest quasihole (red) levels. Upper panel: CPU time versus the number of electrons. The power law fit (solid line) yields an exponent close to 1.

equivalently, the single-particle density matrix). The sGW approximation is a fully quantum paradigm shift and removes the main obstacle for addressing large systems up to the mesoscopic limit. Indeed, the application to silicon NCs of size far exceeding the current state-of-the-art indicates that the complexity is near linear with system size, breaking the theoretical limit. Some of the concepts presented here may be applicable to other forms of MBPT, such as propagator [68] and Green function theories [69].

The sGW method developed here has several appealing advantages: (i) Representation: It is especially suitable for real-space-grid and/or plane-wave pseudopotential representations for which the Hamiltonian operation on a stochastic orbital scales linearly. These representations are natural for large-scale electronic structure computations. The approach is also useful for periodic systems with very large super-cells. (ii) CPU time scaling: The present method enables a GW calculation that scales near linearly in CPU time. Existing methods have been able to reduce the complexity to cubic and it was implicitly assumed that linear scaling is impossible due to the complexity of RPA. The present method circumvents this

by developing sTDH. The scaling of our approach is insensitive to the sparsity of the density matrix and thus represents a significant improvement over existing GW implementations. (iii) Storage scaling (matrix compression): The introduction of the stochastic orbitals circumvents the need to store huge matrices of the Green function and the polarization potential (or the inverse dielectric matrix ϵ^{-1} , etc.), thus achieving considerable savings in memory. The scaling of storage is $O(N_g)$, which makes the sGW calculation applicable to a large system without recourse to various energy cutoff approximations in the unoccupied space [13,70,71]. (iv) Parallelization: The stochastic character of the sGW formalism allows for straightforward parallelization—self-energies are averaged over different stochastic orbitals and each processor performs its own independent contribution to this average.

These features make sGW the method of choice for studying QP excitations in large complex materials not accessible by other approaches.

R. B. and E. R. are supported by The Israel Science Foundation—FIRST Program (Grant No. 1700/14). D. N., Y. G., C. A., and C. K. are part of the Molecularly Engineered Energy Materials (MEEM), an Energy Frontier Research Center funded by the DOE, Office of Science, Office of Basic Energy Sciences under Award No. DE-SC0001342. D. N. and C. A. also acknowledge support by the National Science Foundation (NSF), Grant No. CHE-1112500. Some of the simulations used resources of the Argonne Leadership Computing Facility at Argonne National Laboratory, which is supported by the Office of Science of the U.S. Department of Energy under Contract No. DE-AC02-06CH11357.

- [1] L. Hedin, *Phys. Rev.* **139**, A796 (1965).
- [2] C. Friedrich and A. Schindlmayr, *NIC Series* **31**, 335 (2006).
- [3] A. L. Fetter and J. D. Walecka, *Quantum Theory of Many Particle Systems* (McGraw-Hill, New York, 1971), p. 299.
- [4] M. S. Hybertsen and S. G. Louie, *Phys. Rev. Lett.* **55**, 1418 (1985).
- [5] M. S. Hybertsen and S. G. Louie, *Phys. Rev. B* **34**, 5390 (1986).
- [6] W. G. Aulbur, M. Stadelde, and A. Gorling, *Phys. Rev. B* **62**, 7121 (2000).
- [7] A. Stan, N. E. Dahlen, and R. van Leeuwen, *Europhys. Lett.* **76**, 298 (2006).
- [8] M. Shishkin and G. Kresse, *Phys. Rev. B* **75**, 235102 (2007).
- [9] P. Huang and E. A. Carter, *Annu. Rev. Phys. Chem.* **59**, 261 (2008).
- [10] P. E. Trevisanutto, C. Giorgetti, L. Reining, M. Ladisa, and V. Olevano, *Phys. Rev. Lett.* **101**, 226405 (2008).
- [11] C. Rostgaard, K. W. Jacobsen, and K. S. Thygesen, *Phys. Rev. B* **81**, 085103 (2010).
- [12] P. Liao and E. A. Carter, *Phys. Chem. Chem. Phys.* **13**, 15189 (2011).
- [13] J. A. Berger, L. Reining, and F. Sottile, *Phys. Rev. B* **85**, 085126 (2012).
- [14] M. van Setten, F. Weigend, and F. Evers, *J. Chem. Theory Comput.* **9**, 232 (2013).

- [15] N. Marom, F. Caruso, X. Ren, O.T. Hofmann, T. Körzdörfer, J.R. Chelikowsky, A. Rubio, M. Scheffler, and P. Rinke, *Phys. Rev. B* **86**, 245127 (2012).
- [16] L. Y. Isseroff and E. A. Carter, *Phys. Rev. B* **85**, 235142 (2012).
- [17] S. Refaely-Abramson, S. Sharifzadeh, N. Govind, J. Autschbach, J. B. Neaton, R. Baer, and L. Kronik, *Phys. Rev. Lett.* **109**, 226405 (2012).
- [18] F. Caruso, P. Rinke, X. Ren, A. Rubio, and M. Scheffler, *Phys. Rev. B* **88**, 075105 (2013).
- [19] J. C. Grossman, M. Rohlfing, L. Mitas, S. G. Louie, and M. L. Cohen, *Phys. Rev. Lett.* **86**, 472 (2001).
- [20] G. Onida, L. Reining, and A. Rubio, *Rev. Mod. Phys.* **74**, 601 (2002).
- [21] M. L. Tiago and J. R. Chelikowsky, *Phys. Rev. B* **73**, 205334 (2006).
- [22] S. Refaely-Abramson, R. Baer, and L. Kronik, *Phys. Rev. B* **84**, 075144 (2011).
- [23] F. Caruso, P. Rinke, X. Ren, M. Scheffler, and A. Rubio, *Phys. Rev. B* **86**, 081102 (2012).
- [24] X. Blase, C. Attaccalite, and V. Olevano, *Phys. Rev. B* **83**, 115103 (2011).
- [25] S. V. Faleev, M. van Schilfgaarde, and T. Kotani, *Phys. Rev. Lett.* **93**, 126406 (2004).
- [26] S. Y. Quek, L. Venkataraman, H. J. Choi, S. G. Louie, M. S. Hybertsen, and J. B. Neaton, *Nano Lett.* **7**, 3477 (2007).
- [27] S. Y. Quek, J. B. Neaton, M. S. Hybertsen, E. Kaxiras, and S. G. Louie, *Phys. Rev. Lett.* **98**, 066807 (2007).
- [28] K. S. Thygesen and A. Rubio, *Phys. Rev. B* **77**, 115333 (2008).
- [29] P. Myöhänen, A. Stan, G. Stefanucci, and R. van Leeuwen, *Phys. Rev. B* **80**, 115107 (2009).
- [30] M. Della Sala, F. Angela, G. Kladnik, A. Cossaro, A. Verdini, M. Kamenetska, I. Tamblyn, S. Y. Quek, J. B. Neaton, D. Cvetko, A. Morgante, and L. Venkataraman, *Nano Lett.* **10**, 2470 (2010).
- [31] J. B. Neaton, M. S. Hybertsen, and S. G. Louie, *Phys. Rev. Lett.* **97**, 216405 (2006).
- [32] I. Tamblyn, P. Darancet, S. Y. Quek, S. A. Bonev, and J. B. Neaton, *Phys. Rev. B* **84**, 201402 (2011).
- [33] H.-V. Nguyen, T. A. Pham, D. Rocca, and G. Galli, *Phys. Rev. B* **85**, 081101 (2012).
- [34] J. Deslippe, G. Samsonidze, D. A. Strubbe, M. Jain, M. L. Cohen, and S. G. Louie, *Comput. Phys. Commun.* **183**, 1269 (2012).
- [35] T. A. Pham, H.-V. Nguyen, D. Rocca, and G. Galli, *Phys. Rev. B* **87**, 155148 (2013).
- [36] D. Foerster, P. Koval, and D. Sánchez-Portal, *J. Chem. Phys.* **135**, 074105 (2011).
- [37] X. Gonze *et al.*, *Comput. Phys. Commun.* **180**, 2582 (2009).
- [38] R. Baer and E. Rabani, *Nano Lett.* **12**, 2123 (2012).
- [39] D. Neuhauser, E. Rabani, and R. Baer, *J. Chem. Theory Comput.* **9**, 24 (2013).
- [40] D. Neuhauser, E. Rabani, and R. Baer, *J. Phys. Chem. Lett.* **4**, 1172 (2013).
- [41] R. Baer, D. Neuhauser, and E. Rabani, *Phys. Rev. Lett.* **111**, 106402 (2013).
- [42] Q. Ge, Y. Gao, R. Baer, E. Rabani, and D. Neuhauser, *J. Phys. Chem. Lett.* **5**, 185 (2014).
- [43] L. W. Wang and A. Zunger, *J. Phys. Chem.* **98**, 2158 (1994).
- [44] S. Ogut, J. R. Chelikowsky, and S. G. Louie, *Phys. Rev. Lett.* **79**, 1770 (1997).
- [45] D. Neuhauser, *J. Chem. Phys.* **93**, 2611 (1990).
- [46] See Supplemental Material at <http://link.aps.org/supplemental/10.1103/PhysRevLett.113.076402>, which includes Refs. [3,47,51], for details concerning the exchange calculations.
- [47] M. F. Hutchinson, *Comm. Stat. Simul. Comp.* **18**, 1059 (1989).
- [48] D. A. Drabold and O. F. Sankey, *Phys. Rev. Lett.* **70**, 3631 (1993).
- [49] L. W. Wang, *Phys. Rev. B* **49**, 10154 (1994).
- [50] R. Silver, H. Roeder, A. Voter, and J. Kress, in *Maximum Entropy and Bayesian Methods* (Springer, Berlin, 1996), p. 187.
- [51] R. Kosloff, *J. Phys. Chem.* **92**, 2087 (1988).
- [52] R. Kosloff, *Annu. Rev. Phys. Chem.* **45**, 145 (1994).
- [53] See Supplemental Material at <http://link.aps.org/supplemental/10.1103/PhysRevLett.113.076402>, which includes Refs. [3,47,51], for details of the Chebyshev calculation.
- [54] S. Baroni, S. de Gironcoli, A. Dal Corso, and P. Giannozzi, *Rev. Mod. Phys.* **73**, 515 (2001).
- [55] R. Baer and D. Neuhauser, *J. Chem. Phys.* **121**, 9803 (2004).
- [56] D. Neuhauser and R. Baer, *J. Chem. Phys.* **123**, 204105 (2005).
- [57] E. Runge and E. K. U. Gross, *Phys. Rev. Lett.* **52**, 997 (1984).
- [58] See, Fetter and Walecka [3], Eq. (13.20).
- [59] See Supplemental Material at <http://link.aps.org/supplemental/10.1103/PhysRevLett.113.076402>, which includes Refs. [3,47,51], for details of the stochastic TDH calculations.
- [60] For example, in $\text{Si}_{35}\text{H}_{36}$ the calculated quasielectron energy is -1.93 eV when $N_f = 16$ and -1.86 eV when $N_f = 8$, while for $\text{Si}_{353}\text{H}_{196}$ it is -3.32 eV for both $N_f = 16$ and $N_f = 8$.
- [61] The model system is a SiH_4 molecule represented on a $4 \times 4 \times 4$ grid with a spacing of $1.25a_0$ and in order to get a substantial HOMO-LUMO gap we filled the system with 14 electrons. Given the level of theory, i.e., G_0W_0 on top of LDA and RPA screening, the two methods make no further approximations.
- [62] N. Troullier and J. L. Martins, *Phys. Rev. B* **43**, 1993 (1991).
- [63] L. Kronik, T. Stein, S. Refaely-Abramson, and R. Baer, *J. Chem. Theory Comput.* **8**, 1515 (2012).
- [64] T. Stein, J. Autschbach, N. Govind, L. Kronik, and R. Baer, *J. Phys. Chem. Lett.* **3**, 3740 (2012).
- [65] B. W. Larson, J. B. Whitaker, X.-B. Wang, A. A. Popov, G. Rumbles, N. Kopidakis, S. H. Strauss, and O. V. Boltalina, *J. Phys. Chem. C* **117**, 14958 (2013).
- [66] K. Akaike, K. Kanai, H. Yoshida, J. Tsutsumi, T. Nishi, N. Sato, Y. Ouchi, and K. Seki, *J. Appl. Phys.* **104**, 023710 (2008).
- [67] R. Del Sole, L. Reining, and R. W. Godby, *Phys. Rev. B* **49**, 8024 (1994).
- [68] J. Linderberg and Y. Ohrn, *Propagators in Quantum Chemistry* (John Wiley & Sons, New York, 2004).
- [69] L. Cederbaum and W. Domcke, *Adv. Chem. Phys.* **36**, 205 (1977).
- [70] M. M. Rieger, L. Steinbeck, I. White, H. Rojas, and R. Godby, *Comput. Phys. Commun.* **117**, 211 (1999).
- [71] G. Samsonidze, M. Jain, J. Deslippe, M. L. Cohen, and S. G. Louie, *Phys. Rev. Lett.* **107**, 186404 (2011).